Bridging Innovations in Nanoparticle-based Hyperthermia: From 3D-Engineered Tumor Models to Extracellular Vesicles-Coated Nanoparticles

Aránzazu Villasante[1,2,3]
Gema Quiñonero[1], Juan Gallo[4], Andreia Magalhaes[4], Josep Samitier[1,2,3],
[1]Institute for Bioengineering of Catalonia (IBEC), Baldiri Reixac, 10-12, 08028. Barcelona, Spain
[2]Department of Electronic and Biomedical Engineering, Faculty of Physics, University of Barcelona, Martí i Franquès, 1-11, 08028. Barcelona, Spain.
[3]Biomedical Research Networking Center in Bioengineering, Biomaterials, and Nanomedicine (CIBER-BBN), Av. Monforte de Lemos, 3-5, 28029 Madrid Spain.
[4]International Iberian Nanotechnology Laboratory (INL), Av. Mte. José Veiga s/n, 4715-330. Braga, Portugal

avillasante@ibecbarcelona.eu

Leveraging nanoparticles (NPs) for targeted therapies has shown promise in various cancer types[1,2], yet the pressing need for advanced therapeutic strategies in Neuroblastoma (NB), a prevalent pediatric cancer, remains unmet[1-3]. This gap is partly attributed to the limitations of existing models, including 2D conventional cultures or animal models, which fail to accurately represent human NB[4]. The pivotal factor demanding representation is the tumor microenvironment, encompassing composition, three-dimensionality, and the cellular niche. Consequently, recent research has shifted towards the development of 3-dimensional human tissue-engineered tumor models, aiming for a more faithful recapitulation of tumor features and eliciting human therapeutic responses[5].

In the realm of advanced therapeutic strategies, Magnetic Hyperthermia (MH) and Photothermal Therapy (PTT) stand out as innovative approaches for cancer treatment[6,7]. MH involves superparamagnetic nanoparticles generating heat under an external magnetic field, selectively heating cancer cells[6]. PTT, on the other hand, employs light-absorbing nanoparticles converting light energy into heat upon laser irradiation, leading to localized thermal ablation of cancer cells[7]. Both methods strive for precise and minimally invasive cancer treatment by exploiting the unique properties of nanoparticles in targeted hyperthermic applications[6,7].

This study integrates pioneering concepts in nanoparticle (NP) development, capitalizing on hyperthermia's potential, and harnessing three-dimensional (3D)-engineered tumor models. Additionally, we introduce Extracellular vesicles (EVs) as biomimetic carriers to enhance specific tumor targeting[7,8] and overcome challenges related to the protein corona and immune responses[9,10]. EVs, small membrane vesicles with intrinsic targeting capabilities and low immunogenicity, emerge as an ideal surface coating for obtaining biomimetic NPs[7-11]. This comprehensive approach holds promise for advancing precise and effective neuroblastoma therapies.

Initiating with a focus on optimizing NP internalization in a relevant NB model, we synthesized PAA-functionalized magnetite nanoparticles (Fe3O4@PAA-Rh) and employed a tissue-engineered neuroblastoma (TE-NB) model replicating the native tumor microenvironment. Investigation into Fe3O4@PAA-Rh internalization within NB cells in the TE-NB revealed maximum accumulation overnight, ensuring robust cell viability (Figure 1A); however, low NP internalization was observed.

Exploiting the heightened glucose metabolism in cancer cells, we synthesized glucose-functionalized nanoparticles (Fe3O4@PAA-Rh-Glc). Both hydrodynamic size measurements and ζ-potential values confirmed the successful coupling of glucose (Figures 1B and 1C). Glucose-modified NP exhibited enhanced cellular uptake in the 3D model compared to the counterparts without causing toxicity (Figures 1D and 1E).

Subsequently, we investigated the comparative efficacy of MH and PTT using Fe3O4@PAA-Rh-Glc in the TE-NB model (Figure 2). PTT affected negatively cell proliferation at 24 hours post-treatment in the irradiated central area of the TE-NB model, while in MH the effect was null or positive proliferation. Importantly, After 48 hours post-hyperthermia treatments, MH induced a decrease in proliferation of 20% compared to the untreated control but the PTT-treated samples proliferated higher than the untreated controls. Also, we found that while MH induces a homogeneous reduction of proliferative cells, PTT results in a localized absence of cell proliferation within the irradiated zone. However, neither modality achieves complete tumor eradication, emphasizing the necessity for a strategic combination of therapeutic options.

Expanding on these findings, we studied the use of EVs as carriers for Fe3O4@PAA-Rh-Glc, aiming to improve specific tumor targeting. Figure 3 visually represents the successful integration of Fe3O4@PAA-Rh-Glc into EVs, utilizing a parental labeling method.

As an ongoing facet, the effectiveness of MH and PTT using EV-coated Fe3O4@PAA-Rh-Glc is actively compared. Our research aims to delineate the advantages and limitations of each hyperthermia modality when coupled with EV-coated NPs, contributing valuable insights to the field of nanomedicine and neuroblastoma therapies.

In conclusion, our integrative approach incorporating 3D-engineered tumor models to evaluate NP targeting, uptake, and optimization coupled with hyperthermia modality comparison and strategic EV utilization holds promise for precise and effective neuroblastoma therapies for translational purposes.

References

[1] Xu, M. et al. Cancer Nanomedicine: Emerging Strategies and Therapeutic Potentials. Molecules 28, 5145 (2023).

[2] Mitchell, M. J. et al. Engineering precision nanoparticles for drug delivery. Nat. Rev. Drug Discov. 20, 101–124 (2020).

[3] Matthay, K. K. et al. Neuroblastoma. Nat Rev Primer 2, 16078 (2016).

[4] Krawczyk, E.; Kitlińska, J. Preclinical Models of Neuroblastoma—Current Status and Perspectives. Cancers 2023, 15, 3314

[5] Corallo, D.; Frabetti, S.; Candini, O.; Gregianin, E.; Dominici, M.; Fischer, H.; Aveic, S. Emerging Neuroblastoma 3D In Vitro Models for Pre-Clinical Assessments. Front. Immunol. 2020, 11, 584214.

[6] Włodarczyk, A.; Gorgoń, S.; Radoń, A.; Bajdak-Rusinek, K. Magnetite Nanoparticles in Magnetic Hyperthermia and Cancer Therapies: Challenges and Perspectives. Nanomaterials 2022, 12, 1807

[7] Gallo, J.; Villasante, A. Recent Advances in Biomimetic Nanocarrier-Based Photothermal Therapy for Cancer Treatment. IJMS 2023, 24, 15484

[8] Liu, X., Xiao, C. & Xiao, K. Engineered extracellular vesicles-like biomimetic nanoparticles as an emerging platform for targeted cancer therapy. J. Nanobiotechnology 21, 287 (2023).

[9] Mahmoudi, M., Landry, M. P., Moore, A. & Coreas, R. The protein corona from nanomedicine to environmental science. Nat. Rev. Mater. 8, 422–438 (2023).

[10] Ernst, L., Casals, E., Italiani, P., Boraschi, D. & Puntes, V. The Interactions between Nanoparticles and the Innate Immune System from a Nanotechnologist Perspective. Nanomaterials 11, 2991 (2021).

[11] van Niel, G., D'Angelo, G. & Raposo, G. Shedding light on the cell biology of extracellular vesicles. Nat Rev Mol Cell Biol 19, 213–228 (2018).

Figures

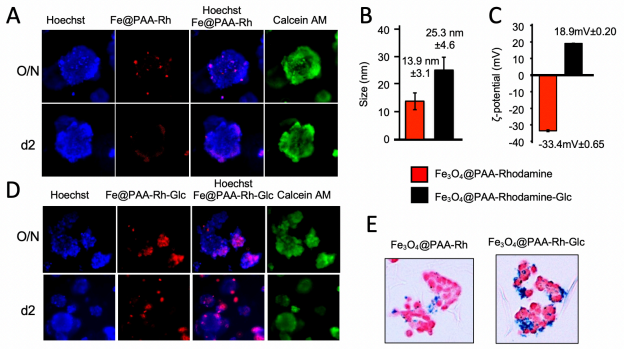

Figure 1. Evaluation of nanoparticle internalization in a 3D neuroblastoma tissue-engineered model (TE-NB). (A) Fluorescence microscopy images capturing the internalization of Fe3O4@PAA-Rh at various time points (O/N= overnight; d2= 2 days). Cell nuclei were stained by Hoechst 33342, and live cells in green by calcein-AM. (B) Hydrodynamic size measurements and (C) ζ-potential values of the indicated nanoparticles confirming the successful coupling of glucose to Fe3O4@PAA-Rh nanoparticles (D) Enhanced Internalization of Glucose-Functionalized Fe3O4@PAA-Rh Nanoparticles in a TE-NB model and cell viability. (E) Prussian blue staining demonstrating the uptake of iron nanoparticles within TE-NB. Representative images are shown (n=6).

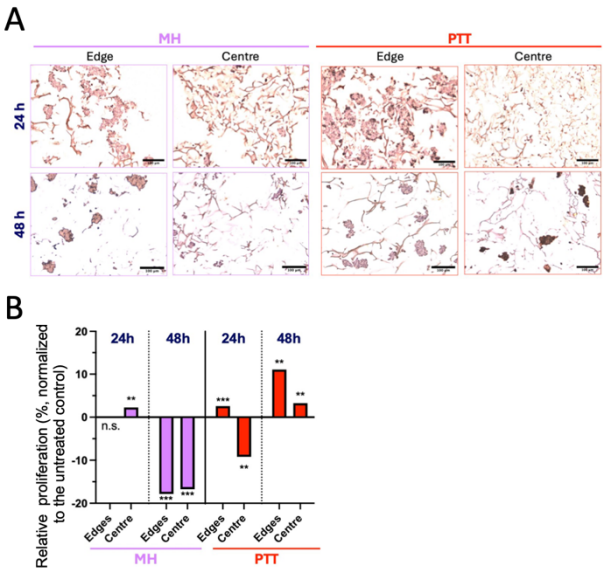

Figure 2. Magnetic Hyperthermia (MH) and Photothermal Therapy (PTT) studies in 3D neuroblastoma tissue-engineered models (TE-NB) treated with Fe3O4@PAA-Rh-Glc nanoparticles. (A) Ki67 staining (in brown) to detect proliferative cells on the edges and in the inner core of the TE-NB models after 24 hours and 48 hours of the indicated treatments. Representative images are shown (n=3). (B) Analysis of the Ki67 staining images. Statistical significance was determined by the two-tailed Student's t test. **p < 0.01; ***p < 0.001; ns, not significant.

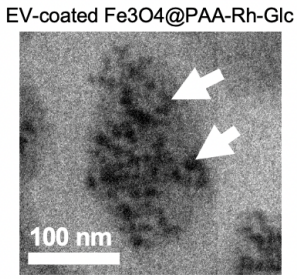

Figure 3. Transmission electron microscopy (TEM) images confirming the presence of Fe3O4@PAA-Rh-Glc within EVs. Representative images of 3 independent assays